Optik 158 (2018) 33–36

Contents lists available at ScienceDirect

Optik

journal homepage: www.elsevier.de/ijleo

Original research article

Reflective solar blind filter based on dielectric multilayer

Xiaodong Wang[a,*], Bo Chen[a], Ling Yao[b]

[a] State Key Laboratory of Applied Optics, Changchun Institute of Optics, Fine Mechanics and Physics, Chinese Academy of Sciences, Changchun 130033, China
[b] Shenyang Aircraft Design and Research Institute, Shenyang 110035, China

ARTICLE INFO

Article history:
Received 19 September 2017
Received in revised form
30 November 2017
Accepted 7 December 2017

Keywords:
Minus filter
Solar blind
LaF_3
MgF_2

ABSTRACT

We report on the design and fabrication of LaF_3/MgF_2 multilayer for use as a reflective solar blind filter. The deposited filter has the average reflectance of 36.5% in 240–280 nm, and it has the average reflectance of 1.8% in 281–760 nm. Reflectance suppression ratio between in-band and out-of-band is 20.3:1.

1. Introduction

Generally, in solar spectrum, 240–280 nm spectral region is called solar blind band. This is because that 240–280 nm lines in solar radiation are totally absorbed by the ozone layer when they go through Earth's atmosphere. This provides an advantage for detecting of solar blind radiation target on Earth surface because the background noise is very low. Detecting of solar blind radiation targets has been widely employed in fire warning [1], corona discharge recognition in electricity transfer [2], missile plume identification [3], chemical/biological sensing [4], convert communication [5].

Reflective SBF is a key optical component in detecting system of solar blind radiation target, and it can provide a high-intensity of output in 240–280 nm, meanwhile, suppression in 281–760 nm. Transmissive SBF has been successfully fabricated [6–11]. Safin et al. designed and fabricated SBF with the transmittance of about 20.0% [6]. Li and Chou prepared SBF with a 27.0% transmission peak consisting of a metal nano-grid by nanoimprint lithography [7]. Kim et al. provided a metal-dielectric multilayer SBF that is relatively insensitive to the incident angle [10]. Al/SiO_2 [9,10], Al/Al_2O_3 [8,10], Ag/SiO_2 [8] stacks were employed to fabricate transmissive SBF. As for reflective SBF, only Zhang et al. theoretically discussed the optimization of reflective MgF_2/Y_2O_3 SBF [12]. To our knowledge, until now, there is no literature about successful fabrication of reflective SBF. In this paper, we report on the design and fabrication of LaF_3/MgF_2 multilayer for use as a reflective SBF.

* Corresponding author.
E-mail address: wangxiaodong@ciomp.ac.cn (X. Wang).

https://doi.org/10.1016/j.ijleo.2017.12.018
0030-4026/

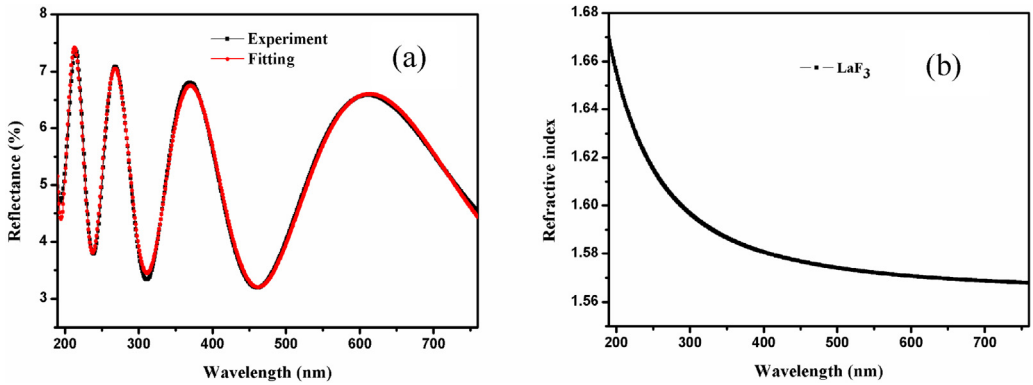

Fig. 1. (a) Fitting of measured reflectance data of a single-layer of LaF_3 with a thickness of 293 nm. (b) Wavelength dependence of the refractive index of LaF_3 films.

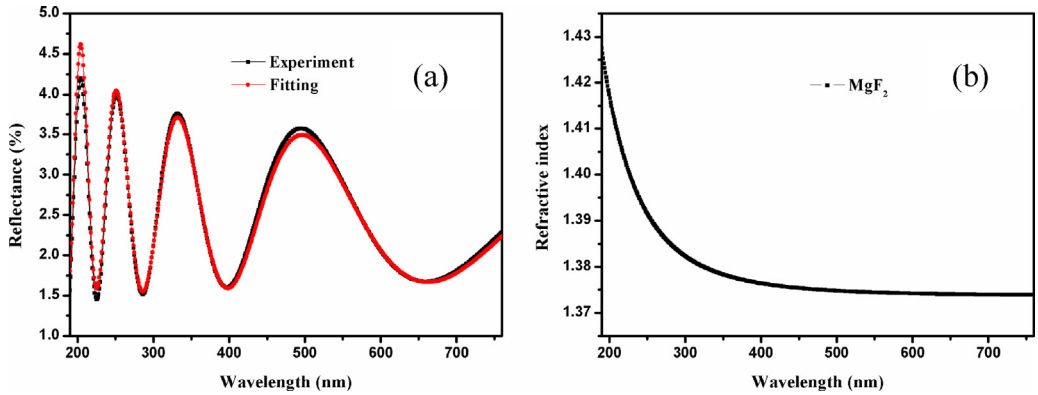

Fig. 2. (a) Fitting of measured reflectance data of a single-layer of MgF_2 with a thickness of 363 nm by model reflectance. (b) Wavelength dependence of the refractive index of MgF_2 films.

2. Design of reflective SBF

LaF_3 and MgF_2 are selected to be high- and low-index material, respectively. The optical constants of LaF_3 and MgF_2 were derived by us from characterization of reflectance for a single-layer by OptiLayer software [13]. Based on literature survey [14–16], it is found that it is reasonable that the refractive index is fitted using normal dispersion model, and the extinction coefficient is fitted using non-absorbing model in 190–760 nm. Normal dispersion model is also called as Cauchy model, and in this model, refractive index of the material is described as the one that decreases with the increasing of wavelength. Cauchy model is described by Eq. (1):

$$n(\lambda) = A_0 + A_1/\lambda^2 + A_2/\lambda^4 \tag{1}$$

where n is refractive index, A_0–A_2 are constants, and λ is wavelength. Non-absorbing model means that in this model, extinction coefficient of the material is zero.

The reflectance of the single layer of LaF_3 and MgF_2 was characterized by Lambda 1050 Spectrophotometer with a step of 1 nm in ambient atmosphere, and the incident angle is 6°. Fig. 1(a) shows fitting of measured reflectance data of a single-layer of LaF_3 with a thickness of 293 nm, and the inhomogeneity is −2.0%; Fig. 1(b) shows wavelength dependence of the refractive index of LaF_3 films, and it is closed to that reported in Ref.14 (sample of EB, deviation of 1.2%) and 15 (deviation of 4.2%), which indicates our results are reliable. Fig. 2(a) shows fitting of measured reflectance data of a single-layer of MgF_2 with a thickness of 363 nm by model reflectance, and the inhomogeneity is −0.2%; Fig. 2(b) shows wavelength dependence of the refractive index of MgF_2 films, and it is very similar to that reported in Ref.15 (deviation of 0.7%) and 16 (sample of 250°, deviation of 0.4%), which indicates that our results are reliable.

A traditional quarter-wave (QW) periodic multilayer and two non-periodic stacks optimized by two methods are designed. Optimized multilayer I is obtained utilizing Constrained Optimization in OptiLayer software, and Optimized multilayer II is obtained using Sensitivity-Directed Refinement in OptiLayer software. In Constrained Optimization, It is capable of setting constraints for individual layer thicknesses, and each layer can be specified whether the thickness of this layer can vary during optimization. The lower and upper thickness limits are set to be 10 nm and 100 nm, respectively, and all the layers vary during optimization I. In Sensitivity-Directed Refinement, based on the calculation of design sensitivity to

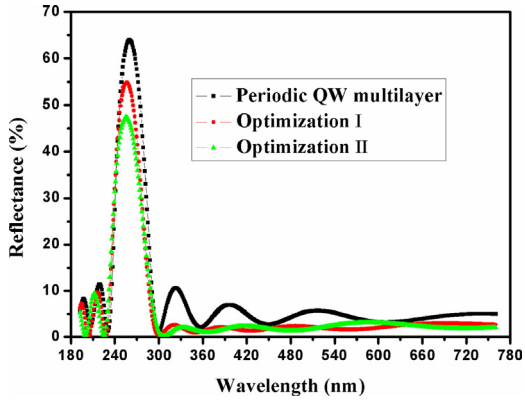

Fig. 3. Design results of reflective SBF. The substrate is fused silica, and the incident angle is 6°.

Table 1
Summary of properties of our design.

Item	QW periodic multilayer	Optimization I	Optimization II
$R_{240\text{-}280}$	53.7%	44.9%	39.5%
$R_{281\text{-}760}$	4.7%	2.1%	2.0%
Suppression ratio	11.4:1	21.4:1	19.8:1

Table 2
Design results ofoptimization multilayer II.

Layer number	1	2	3	4	5	6	7	8	9	10	11	12	13
Thickness (nm)	10.0	14.5	52.7	31.2	40.0	49.5	35.2	47.6	43.7	36.8	43.0	72.3	10.0

layer thickness variations, a given number of most sensitivity layers released are further refined, Needle Optimization is also utilized in each optimization after each iteration. In Optimization I and II, thickness of each layer is the variable that needs to be optimized; the target of this optimization is: a reflectance of 60% in 240–280 nm, a reflectance of zero in 190–237 nm and 290–760 nm. Fig. 3 demonstrates our design results of reflective SBF, the substrate is fused silica, and the incident angle is 6°. Traditional QW periodic multilayer has the highest average reflectance of 53.7% in 240–280 nm, the mean reflectance is 4.7% in 281–760 nm, and the suppression ratio between in-band and out-of-band is 11.4:1; Optimized multilayer I has the average reflectance of 44.9% in 240–280 nm, the mean reflectance is 2.1% in 281–760 nm, and the suppression ratio is 21.4:1; Optimized multilayer II has the average reflectance of 39.5% in 240–280 nm, the mean reflectance is 2.0% in 281–760 nm, and the suppression ratio is 19.8:1. It can be found that after optimization, the suppression ratio of non-periodic multilayer improves significantly. Table 1 summarizes the properties of our design. Although the properties of optimization multilayer I are better than optimization multilayer II, there are several MgF_2 layers with thickness of larger than 70 nm. Electron beam will dig a big hole when a thicker MgF_2 layer is deposited, which will result in a big error in thickness control. Thus, optimization multilayer II is chosen to be deposited. Table 2 demonstrates thickness of each layer in optimization multilayer II. The first layer is near to the substrate, the odd layer is LaF_3 film, the even layer is MgF_2 film.

3. Fabrication of reflective SBF

The used LaF_3 and MgF_2 have a purity of 99.99%. The depositions were made in an electron beam evaporation vacuum chamber. The base pressure was 3.0×10^{-4} Pa. LaF_3 was evaporated by heated resistance boat, and MgF_2 in copper crucible was evaporated by electron beam. The voltage of electron gun was fixed to be 10 kV, the thickness of films and deposition rate were controlled by a quartz crystal (IC6, Inficon Company). The distance between the source and substrate is 50 cm, the distance between the quartz crystal and source is 45 cm. The deposition rate of LaF_3 and MgF_2 was 0.5 nm/s. The fused silica substrate was heated to be 250° prior to deposition.

The reflectance of films in the wavelength range of 185–760 nm was characterized by Lambda 1050 UV/VIS/NIR Spectrophotometer with a step of 1 nm in ambient atmosphere, and the incident angle is 6°. Relative reflectance measurement method is utilized in our reflectance characterization, Si substrate is used as a standard, and the spot size is 5 mm × 5 mm.

Fig. 4 shows experimental result of reflective SBF, for comparison, theoretical design (optimization II) is also presented, and the incident angle is 6°. The fabricated SBF has the average reflectance of 36.5% in 240–280 nm, the mean reflectance is 1.8% in 281–760 nm, and the suppression ratio between in-band and out-of-band is 20.3:1. Experimental result shows good agreement with theoretical design.

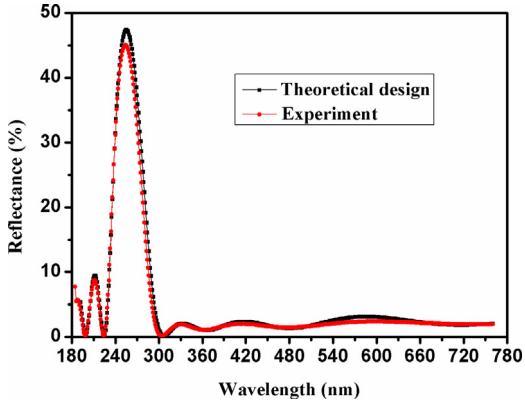

Fig. 4. Experimental and theoretical results of reflective SBF.

4. Conclusion

A reflective SBF was successfully designed and fabricated. This optimized non-periodic multilayer has the mean reflectance of 36.5% in the working spectral range, the average reflectance is 1.8% in longer wavelength and visible line, and the suppression ratio between in-band and out-of-band is 20.3:1.

Acknowledgments

This work is partially supported by the Joint Research Fund in Astronomy (U1531106) under cooperative agreement between the National Natural Science Foundation of China (NSFC) and Chinese Academy of Science (CAS). We thank Professor Alexander Tikhonravov from Moscow State University for fruitful discussions of characterization of optical constant of MgF_2 films.

References

[1] T. Oshima, T. Okuno, N. Arai, N. Suzuki, H. Hino, S. Fujita, Flame detection by a beta-Ga_2O_3-based sensor, Jpn. J. Appl. Phys. 48 (1) (2009) 011605.
[2] E.V. Gorokhov, A.N. Magunov, V.S. Feshchenko, A.A. Altukhov, Solar-blind UV flame detector based on natural diamond, Instrum. Exp. Tech. 51 (2) (2008) 280–283.
[3] M. Razeghi, A. Rogalski, Semiconductor ultraviolet detectors, J. Appl. Phys. 79 (1996) 7433–7473.
[4] A.Y. Hudeish, C.K. Tan, A.A. Aziz, Z. Hassan, A chemical sensor based on AlGaN, Funct. Mater. Devices 517 (2006) 33–36.
[5] G. Chen, Z.Y. Xu, H.P. Ding, B.M. Sadler, Path loss modeling and performance trade-off study for shortrange non-line-of-sight ultraviolet communications, Opt. Express 17 (5) (2009) 3929–3940.
[6] R.G. Safin, I.S. Gainutdinov, R.S. Sabirov, M.K. Azamatov, Solar-blind filter for the ultraviolet region, J. Opt. Technol. 74 (3) (2007) 208–210.
[7] W.D. Li, S.Y. Chou, Solar-blind deep-UV band-pass filter (250–350 nm) consisting of a metal nano-grid fabricated by nanoimprint lithography, Opt. Express 18 (2) (2010) 931–937.
[8] J. Mu, P.T. Lin, L. Zhang, J. Michel, L.C. Kimerling, F. Jaworski, A. Agarwa, Design and fabrication of a high transmissivity metal-dielectric ultraviolet band-pass filter, Appl. Phys. Lett. 102 (2013) 213105.
[9] T.J. Wang, W.Z. Xu, H. Lu, F.F. Ren, D.J. Chen, R. Zhang, Y.D. Zheng, Solar-blind ultraviolet band-pass filter based on metal-dielectric multilayer structures, Chin. Phys. B 23 (7) (2014) 074201.
[10] S. Kim, M. Man, M. Qi, K.J. Webb, Angle-insensitive and solar-blind ultraviolet bandpass filter, Opt. Lett. 39 (19) (2014) 5784–5787.
[11] J. Hennessy, A.D. Jewell, M.E. Hoenk, S. Nikzad, Metal–dielectric filters for solar–blind silicon ultraviolet detectors, Appl. Opt. 54 (11) (2015) 3507–3512.
[12] H. Zhang, H.H. Jia, J. Yang, S. Chang, H. Ying, The optimization of solar blind UV high reflectance coatings, Proc. SPIE 6781 (2007) 67813J.
[13] A.V. Tikhonravov, M.K. Trubetskov, OptiLayer Thin Film Software http://www.optilayer.com.
[14] G. Liu, H. Yu, W. Zhang, Y. Jin, H. He, Z. Fan, Comparision study of microstructure, chemical composition and optical properties between resistive heating and electron beam evaporated LaF_3 thin films, Thin Solid Films 519 (2011) 3487–3491.
[15] C. Xue, K. Yi, C. Wei, J. Shao, Z. Fan, Optical constants of DUV/UV fluoride thin films, Chin. Opt. Lett. 7 (2009) 449–451.
[16] J. Sun, J. Shao, K. Yi, W. Zhang, Effects of substrate temperatures on the characterization of magnesium fluoride thin films in deep-ultraviolet region, Appl. Opt. 53 (2014) 1298–1305.